Automated construction of monochromatic monitoring strategies

M. Trubetskov,[1,2,*] T. Amotchkina,[2] and A. Tikhonravov[2]

[1]Max-Planck Institute of Quantum Optics, Hans-Kopfermann-Str. 1, 85748 Garching, Germany

[2]Research Computing Center, Moscow State University, Leninskie Gory, 119991 Moscow, Russia

*Corresponding author: Michael.Trubetskov@mpq.mpg.de

Received 9 December 2014; revised 28 January 2015; accepted 28 January 2015;
posted 29 January 2015 (Doc. ID 229323); published 3 March 2015

We focus our efforts on development of an advanced monochromatic monitoring strategy to assist the optical coating engineer in finding a single wavelength or a sequence of monitoring wavelengths that meet simultaneously several practical demands, namely, specified input and output swing values, specified amplitude of a monitoring signal variation, and the distance between trigger point and the last signal extremum. Additionally, the most important demand is that the number of different monitoring wavelengths must be as small as possible. Manual construction of such a monitoring strategy is almost impossible because of a large number of conditions to be satisfied. We propose an algorithm that automatically generates a monitoring spreadsheet so that all demands can be satisfied as closely as possible. We consider six typical design problems and obtain a series of solutions for each of them. Then, we provide computational simulations of deposition processes assuming that they are controlled by monochromatic monitoring with the monitoring strategy generated by our algorithm, and we demonstrate how an optical coating engineer can select design solutions that exhibit the highest production yields.

OCIS codes: (310.1860) Deposition and fabrication; (310.6860) Thin films, optical properties; (310.4165) Multilayer design; (310.6805) Theory and design.

http://dx.doi.org/10.1364/AO.54.001900

1. Introduction

Accurate monitoring of layer thicknesses is the key element of modern multilayer coatings production. It is not surprising that there exists a vast variety of monitoring techniques, and many papers on this subject have been published. The most recent review of the main optical monitoring techniques and their features can be found in Ref. [1]. Many modern optical monitoring systems are represented as a combination of a spectrophotometric device providing *in situ* measurements and a specific monitoring algorithm for analyzing obtained data. Recently, substantial progress has been made in the development of monitoring systems, allowing one to control the deposition of complicated multilayers consisting of several dozen layers.

In the past decades, broadband optical monitoring (BBM) systems have become more and more popular [2–5]. Along with BBM, monochromatic optical monitoring remains a powerful tool in optical coating production [6–12]. The ability to produce challenging multilayer coatings using monochromatic monitoring systems has been demonstrated in Refs. [9,10,12], where dielectric mirrors, antireflection (AR) coatings, cut filters, polarizers, multicavity bandpass filters, and notch filters were produced. These achievements have encouraged us to continue the studies of monochromatic monitoring started in Refs. [13–15].

In our present and previous studies we consider monitoring strategies utilizing level monitoring [16,17]. These strategies require specification of a monitoring wavelength and a termination level (TL) of the monitoring signal for each coating layer. The TL of the monitoring signal (transmittance or reflectance) determines the instant [trigger point -(TP)] at which layer deposition should be terminated. A sequence

1559-128X/15/081900-10$15.00/0

of monitoring wavelengths and corresponding TLs form a monitoring spreadsheet. This spreadsheet may also include other useful information, such as signal amplitude, and maxima and minima values of the monitoring signal during layer deposition. Various algorithms for specification of monitoring spreadsheets have been proposed by several authors. One of the possibilities is to choose the most sensitive wavelength for each coating layer, i.e., the wavelength at which the measured spectral characteristic is most sensitive to variations of the layer thickness at the end of layer deposition [18–20].

Monochromatic monitoring strategies based on level monitoring can be further subdivided into passive and active monitoring strategies [1]. The first term is applied to the strategies that are entirely specified before starting a deposition, and specified TLs are not changed during coating production. In contrast, active strategies explore the on-line information for correcting TLs. A passive strategy based on a special choice of monitoring spreadsheet was proposed in [14]. For this strategy monitoring wavelengths are chosen in such a way that allows reduction of the effect of accumulation of thickness errors. An active strategy proposed in [13] and further studied in [15] was aimed at eliminating the cumulative effect of thickness errors. It includes additional requirements to specification of a monitoring spreadsheet in order to increase the reliability of the proposed real-time control algorithm incorporated into the optical monitoring system [15]. Other examples of active monochromatic monitoring strategies can be found in [19,21].

There exists a large variety of monochromatic monitoring strategies. Specification of monitoring spreadsheets for these strategies is typically based on various empirical suggestions and on the experience of optical coating engineers. Often, these suggestions are connected with technological features of monitoring systems and deposition plants. Generally, it is not a straightforward task to find a good monitoring strategy and a proper monitoring spreadsheet for complicated multilayers. Furthermore, it is known that different design solutions may exhibit different sensitivity to deposition errors. Actually, this means that the problem is even more complicated: not only a monitoring strategy, but also a combination *design–strategy* should be properly selected. This requires a number of trial deposition runs as well as software simulations of real runs [10,22,23]. Essential progress in this direction can be achieved only if empirical specification of monitoring spreadsheets is replaced by a robust automated procedure. Such a procedure should incorporate the main considerations that are usually employed by experienced optical coating engineers in their practice.

The algorithm proposed in this work is, first, aimed at specification of active monochromatic monitoring strategies that explore corrections of TLs based on registered extrema of the monitoring signal. One of the considerations incorporated into the proposed algorithm is the requirement to limit the number of different monitoring wavelengths. The monitoring signal should satisfy also additional practical criteria including limitations for a signal swing, amplitude of a signal variation between adjacent extrema values, and deviations between a TL and an adjacent signal extremum value.

The proposed algorithm takes into account several practical criteria simultaneously. It allows one to weight different requirements and provides a sequence of monitoring wavelengths so that the maximum of these requirements are satisfied. In Section 2 we describe the proposed algorithm. In Section 3 we demonstrate its application to a choice of monitoring strategy for AR coating that should work in a wide range of incidence angles. In Section 4 we apply the novel algorithm in a wide series of computational manufacturing experiments aimed at coordinated selection of a *design–monitoring strategy* for a series of complicated multilayer systems. Our conclusions are presented in Section 5.

2. Description of the Monochromatic Monitoring Strategies Construction Algorithm

In order to describe the novel algorithm, some definitions should be introduced. The *amplitude* of the monitoring signal is the difference between its maximum $V_{\max}$ and minimum $V_{\min}$:

$$A = V_{\max} - V_{\min}. \tag{1}$$

In the case that signal extrema are not achieved during layer deposition (for example, a layer is too thin), then in Eq. (1) we consider virtual increase of its thickness until both extrema are finally located. Examples of computations will be presented below.

Initial and *final signal swings* (S_{in} and S_{fin}) are defined for each coating layer and calculated as follows:

$$S_{\text{in}} = \begin{cases} \frac{V_{\max} - V_{\text{in}}}{A} 100\% & \text{if the first extremum is maximum,} \\ \frac{V_{\text{in}} - V_{\min}}{A} 100\% & \text{otherwise,} \end{cases}$$

$$S_{\text{fin}} = \begin{cases} \frac{V_{\max} - V_{\text{fin}}}{A} 100\% & \text{if the last extremum is maximum,} \\ \frac{V_{\text{fin}} - V_{\min}}{A} 100\% & \text{otherwise,} \end{cases} \tag{2}$$

where V_{in} is the signal level at the start of the layer deposition, and V_{fin} is the TL. Conditions in Eq. (2) require an additional explanation. If at least one extremum is located inside the layer under consideration, the terms "first extremum" and "last extremum" in Eq. (2) are obviously related to one of these extrema, ordered in the direction from substrate to incident medium. In the case of a thin layer, having no extrema of the monitoring signal inside, the conditions are more complicated. It is necessary to consider continuously increasing thickness of the monitored layer above its nominal thickness until the next two extrema appear on the monitoring curve. These two extrema should be considered as the first and

the last ones in the conditions of Eq. (2). Evidently, swing values close to 0% and 100% mean that a signal is close to extremum values. The initial swing for the first layer is always equal to zero.

Another important parameter is the difference between the termination level V_{fin} and the next signal extremum E_{next}:

$$\Delta = |V_{\text{fin}} - E_{\text{next}}|. \tag{3}$$

To calculate this value, virtual extrema are used (see example below).

The proposed algorithm chooses monitoring wavelengths in order to satisfy the following five monitoring conditions (MCs):

MC1. The number of monitoring wavelength changes does not exceed five. The actual number of different monitoring wavelength changes, the allowed spectral range for their choice, and the wavelength grid step for this choice are specified by an optical coating engineer.
MC2. $a_1 \le S_{\text{in}} \le a_2$; the initial swing should be not too small and not too high (the first layer with $S_{\text{in}} = 0$ should be excluded).
MC3. $b_1 \le S_{\text{fin}} \le b_2$; the final swing should be not too small and not too high.
MC4. $A \ge \varepsilon$; the signal amplitude should be not too small.
MC5. $\Delta \ge \delta$; the distance between TL and the next virtual extremum should not be too small.

The values a_1, a_2, b_1, b_2, ε, and δ are the parameters of the algorithm. For example, reasonable values of these parameters are $a_1 = a_2 = 15\%$, $b_1 = b_2 = 85\%$, $\varepsilon = 4\%$, and $\delta = 4\%$. Conditions MC2 and MC3 are connected with the requirement that TL points should be located at signal slopes with enough steepness.

Generally, it may be not possible to find a sequence of wavelengths so that all conditions MC2–MC5 are satisfied simultaneously for all coating layers. Our algorithm chooses monitoring wavelength(s) so that conditions MC2–MC5 are satisfied as closely as possible. It may happen that some conditions are more important than the others. For such cases, condition weights are introduced. The weights allow one to adjust the relative importance of different conditions.

From the mathematical point of view, the search for monitoring wavelengths is based on the optimization of the *monitoring function* F_M:

$$\begin{aligned} F_M = {} & w_{\text{in}}[q(a_1 - S_{\text{in}}) + q(S_{\text{in}} - a_2)] \\ & + w_{\text{fin}}[q(b_1 - S_{\text{fin}}) + q(S_{\text{fin}} - b_2)] \\ & + w_A q(\varepsilon - A) + w_\Delta q(\delta - \Delta), \end{aligned} \tag{4}$$

where $q(x) = x^2$ if $x \ge 0$ and $q(x) = 0$ if $x < 0$. The terms in the expression Eq. (4) are penalty terms for violation of (MC2)-(MC5), correspondingly, with weight factors w_{in}, w_{fin}, w_A, and w_Δ that are also the parameters of the algorithm. Since the number of monitoring wavelength changes is also specified in MC1, we consider all possible combinations of monitoring wavelengths at the given wavelength grid λ_i and compute monitoring function F_M for each of them. The combination of monitoring wavelengths that provides the minimum value of F_M is the monitoring strategy sought. Therefore, the novel monitoring spreadsheet construction algorithm belongs to the exhaustive search algorithm class. The computational time grows rapidly with an increase in the number of allowed monitoring wavelength changes, but for practically important cases (MC1) the computational time is from several seconds up to several dozen of seconds at a modern 2–4 core CPU.

Let us illustrate the algorithm application using a simple example, namely, a model coating consisting of two layers on a Suprasil substrate. Let us take layer refractive indices equal to 2.35 and 1.45, and layer physical thicknesses equal to 150 and 100 nm. Let the monitoring wavelength be 500 nm. The corresponding monitoring signal with indications of maxima, minima, TLs, and virtual extrema is shown in Fig. 1(a). The MC parameters are calculated for Layer 1 as

$$\begin{aligned} A &= 93.21\% - 64.63\% = 28.58\% > \varepsilon = 4\%, \\ S_{\text{in}} &= 0(\text{excluded}), \\ S_{\text{fin}} &= \frac{93.21\% - 66.21\%}{28.58\%} \cdot 100\% = 94.47\% > a_2 = 80\%, \\ \Delta &= 66.21\% - 64.63\% = 1.58\% < \delta = 4\%, \end{aligned} \tag{5}$$

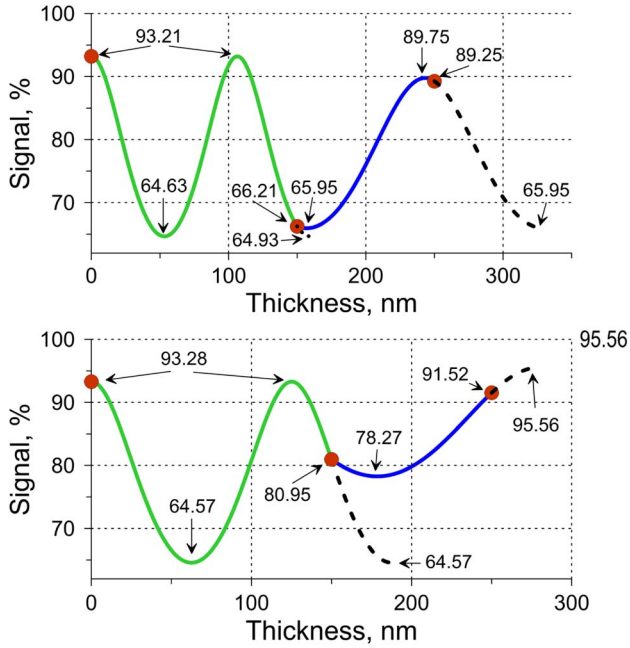

Fig. 1. Illustration of the description of the new strategy: monitoring signals correspond to control wavelengths of 500 nm (upper panel) and 588 nm found by the novel robust strategy (lower panel). The green and blue lines correspond to monitoring signals of the first and second layers. The dashed curves show the virtual monitoring signal corresponding to a virtual increase of layer thickness.

and for Layer 2 as

$$A = 89.75\% - 65.95\% = 23.8\% > \varepsilon = 4\%,$$
$$S_{\text{in}} = \frac{66.23\% - 65.95\%}{23.8\%} \cdot 100\% = 1.2\% < a_1 = 20\%,$$
$$S_{\text{fin}} = \frac{89.75\% - 89.25\%}{23.8\%} = 2.1\% < a_1 = 20\%,$$
$$\Delta = 89.25\% - 65.95\% = 23.3\% > \delta = 4\%. \quad (6)$$

Equations (5) and (6) show that for the first layer condition MC4 is satisfied, and conditions MC3 and MC5 are violated; for the second layer conditions MC4 and MC5 are satisfied, and conditions MC2 and MC3 are violated. As it is seen from Fig. 1(a), the TLs are very close to signal extrema.

Application of our algorithm described above gives a monitoring wavelength of 588 nm. The corresponding monitoring signal is shown in Fig. 1(b). The MC parameters are now for Layer 1 as follows:

$$A = 93.28\% - 64.57\% = 28.71\% > \varepsilon = 4\%,$$
$$S_{\text{in}} = 0(\text{excluded}),$$
$$b_1 = 15\% \le S_{\text{fin}} = \frac{93.28\% - 80.95\%}{28.71\%} \cdot 100\% = 42.9\% < b_2 = 85\%,$$
$$\Delta = 80.95\% - 64.57\% = 16.38\% > \delta = 4\%, \quad (7)$$

and for Layer 2

$$A = 95.56\% - 78.27\% = 17.29\% > \varepsilon = 4\%,$$
$$a_1 = 15\% < S_{\text{in}} = \frac{80.95\% - 78.27\%}{17.29\%} \cdot 100\% = 15.5\% < a_2 = 85\%,$$
$$b_1 = 15\% < S_{\text{fin}} = \frac{91.52\% - 78.27\%}{17.29\%} = 76.6\% < b_2 = 85\%,$$
$$\Delta = 95.56\% - 91.52\% = 4.04\% > \delta = 4\%. \quad (8)$$

It follows from Eqs. (7) and (8) that for both layers all conditions from (MC2) to (MC5) are satisfied.

3. Application of the New Strategy to Monitoring AR Coating

Let us consider an eight-layer AR coating working in the spectral range from 650 to 750 nm, and in angular range from 0 to 70 deg. Light is nonpolarized, and back side reflectance is not taken into account in the course of the design process. The substrate is Suprasil, and the layer materials are Nb_2O_5 and SiO_2 [24]. Refractive indices of all materials are described by thee Cauchy formula $n(\lambda) = A_0 + A_1(\lambda_0/\lambda)^2 + A_2(\lambda_0/\lambda)^4$, where $A_0 = 2.218485$, $A_1 = 0.021827$, and $A_2 = 4 \cdot 10^{-3}$ for Nb_2O_5; $A_0 = 1.465294$, $A_1 = 0$, and $A_2 = 4.71 \cdot 10^{-4}$ for SiO_2; and $A_0 = 1.448442$, $A_1 = 3.129773 \cdot 10^{-3}$, and $A_2 = 3.775 \cdot 10^{-5}$ for Suprasil. If λ is measured in nanometers, then $\lambda_0 = 1000$ nm. AR design layer thicknesses are presented in Table 1. Reflectance in the working spectral and angular ranges does not exceed 9.2%.

First, let us choose as a monitoring wavelength the wavelength of 700 nm located in the middle of the AR spectral range. The corresponding signal is depicted in Fig. 2(a); monitoring extrema, virtual extrema, and trigger points are shown in the fourth column of Table 1. For better visualization we show initial signal value in black, signal minima in green, and signal maxima in red. On the basis of Eqs. (2), amplitude values, initial and final swing values, and distances between TPs and the next turning points are calculated (see columns 5–8 of Table 1). The pink values indicate values that do not satisfy conditions MC2–MC5 with parameters $a_1 = b_1 = 20\%$, $a_2 = b_2 = 80\%$, $\delta = 4\%$, and $\varepsilon = 4\%$. It is seen that only in the first and fifth layers are all conditions MC2–MC5 satisfied. In other layers, at least one condition MC2–MC5 is violated.

In Fig. 3 we show dependence of the F_M function on the monitoring wavelength. It is easy to find that this function takes a minimum value at a wavelength of 621 nm. The corresponding monitoring signal is plotted in Fig. 2(b), and the monitoring spreadsheet is presented in Table 2. Calculated values of monitoring parameters are shown in columns 5–8 of Table 2. It is seen from Table 2 that, in the first layer, conditions MC3 and MC5 are violated, in the second layer only condition MC2 is violated, and in the fifth layer only condition MC3 is violated. As it has been

Table 1. Monitoring Spreadsheet of AR Design (Control Wavelength 700 nm)

Layer number	Material	D_Σ, nm	Response	A, %	S_{in}, %	S_{fin}, %	Δ, %
1	H	49.93	93.36 72.36 66.73	26.63	–	78.9	5.63
2	L	53.86	72.36 71.26 74.62 93.24	21.98	5.0	15.31	18.62
3	H	50.46	74.62 95.62 91.94 60.38	35.24	59.59	10.44	31.56
4	L	91.29	91.94 85.35 86.20 96.52	11.17	58.99	7.61	10.32
5	H	146.60	86.20 89.32 73.84 84.17 89.32	15.48	20.16	66.73	5.15
6	L	202.49	84.17 96.55 83.61 83.22	13.33	97.15	97.07	0.39
7	H	113.23	83.61 76.94 86.46 87.05	10.11	65.97	94.16	0.59
8	L	108.21	86.46 96.41 96.42	9.96	99.8	99.92	0.01

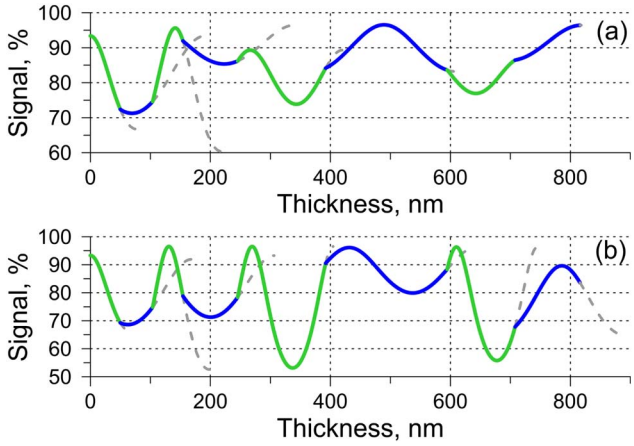

Fig. 2. AR design monitoring curves corresponding to (a) 700 and (b) 621 nm. The green and blue lines are related to the monitoring signal inside the high- and low-index layers, respectively. The gray dashed lines show the theoretical signal expected if the corresponding layer deposition continues without interruption until the next extremum.

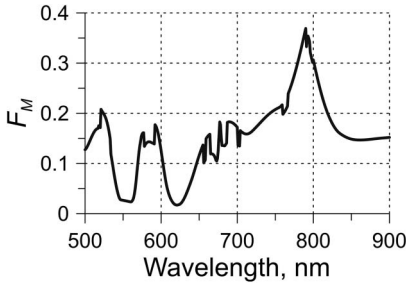

Fig. 3. Dependence of the F_M function on the monitoring wavelength.

mentioned above, one should not expect that it would be always possible to find monitoring wavelengths so that conditions MC2–MC5 are satisfied simultaneously.

To compare monitoring wavelengths of 700 and 621 nm from the practical point of view, we perform a series of computational manufacturing experiments in order to estimate production yields that can be provided with monitoring at these wavelengths. As an estimation of the production yield Y, the ratio of successful and total simulated runs can be taken. To distinguish between successful and unsuccessful deposition runs, the range targets are to be introduced [25]. For our AR design problem, the range target is defined as $R \leq 9.5\%$ in the spectral range from 650 to 750 nm.

In the course of simulations all main sources of deposition errors have been taken into account. In the monochromatic monitoring simulator incorporated into OptiLayer Thin Film Software [26], deposition process instabilities are described by fluctuations of the deposition rates, systematic and random errors in refractive indices, noise of measurement *in situ* transmittance/reflectance data, shutter delay and its fluctuations, and calibration drift of the monitoring signal. In our simulation experiments we took the same numerical values of the deposition parameters as in Ref. [10]. Those parameters are: deposition rates were taken equal to 0.5 and 0.8 nm/s, their fluctuations of 5% and 10% for high- and low-index materials, respectively; systematic and random errors in high refractive index of 1% and 0.5%, respectively; average shutter delay and its fluctuation of 0.5 and 0.1 s, respectively; noise in measurement transmittance signal of 0.015%; and time interval between measurements of 1 s. Additionally, we specified calibration drifts of the monitoring transmittance signal of 0.01% with correlation time of 5 s.

Here and in the computational manufacturing experiments of the next section we use an active monochromatic monitoring strategy that performs correction of TLs—the algorithm that we call the "Simple correction" algorithm. This algorithm performs a shift of TL value equal to the deviation of the last detected extremum value from the theoretical one.

We performed 1000 simulation experiments for each monitoring wavelength. Production yields for wavelengths of 700 and 621 nm are estimated as 0.2% and 98.6%, respectively. It follows from these estimations that the novel algorithm allows one to specify the monitoring strategy that provides a high production yield. At the same time, monitoring at the wavelength of 700 nm gives a yield close to zero.

Table 2. Monitoring Spreadsheet of AR Design (Control Wavelength 621 nm)

Layer number	Material	D_Σ, nm	Response	A, %	S_{in}, %	S_{fin}, %	Δ, %
1	H	49.93	93.32 69.20 66.04	27.28	0	88.44	3.16
2	L	53.86	69.20 68.59 74.90 91.90	23.31	2.6	27.06	17.00
3	H	50.46	74.90 96.54 78.51 52.48	44.06	49.1	40.92	26.03
4	L	91.29	78.77 71.30 78.40 93.27	22.10	33.7	32.77	14.86
5	H	146.60	78.31 96.54 52.77 90.81 96.54	43.75	41.7	86.91	5.73
6	L	202.49	90.81 96.14 79.86 88.73 96.14	16.28	32.7	54.47	7.41
7	H	113.23	88.70 96.39 55.25 67.97 96.39	40.90	18.7	30.92	28.42
8	L	108.21	67.97 89.61 83.15 64.74	24.87	87.8	25.97	18.41

4. Selection of the Best Design–Monitoring-Strategy Combinations

In the example considered in the previous section, the design has only eight layers. In principle, it is possible to select a proper monitoring wavelength manually. This can be done by varying the monitoring wavelength with subsequent visual or numerical estimations of parameters specified by conditions MC2–MC5. In the case of complicated design consisting of dozen of layers, such an approach is not realistic. First of all, it is not evident what number of the monitoring wavelengths should be taken. An exhaustive search of wavelength combinations may take a long time. Second, with the growing number of design layers it becomes more and more difficult to distinguish between favorable or unfavorable combinations of parameters specified by MC2–MC5. The time required for the selection of monitoring wavelengths increases also with the growing number of possible designs that can be used as solutions to the considered design problem. In this section we demonstrate an application of the novel algorithm to the selection of the *design–monitoring-strategy* combination that provides the highest production yield. Six different examples are considered and the best results are collected and summarized in Table 3.

A. Example 1

Consider designing a cold mirror (CM). Target transmittance is 0% and 100% in the spectral ranges [400; 690] nm and [710; 1200] nm, respectively. In this and all other examples we take the same materials and substrate as in Section 3. The design process is based on the minimization of the standard merit function [27]:

$$MF^2 = \frac{1}{L}\sum_{\{\lambda_j\}}\left(\frac{T(X,\lambda_j) - \hat{T}(\lambda_j)}{\Delta T_j}\right)^2, \qquad (9)$$

where X is the vector of layer thicknesses, $T(X,\lambda_j)$ is transmittance of the current design, $\hat{T}(\lambda_j)$ is the target transmittance, $\{\lambda_j\}$ is the wavelength grid in the target spectral range, and $j = 1,\ldots,L$, and ΔT_j are tolerances.

For this design problem, a set of 10 solutions has been obtained. To obtain these solutions, various modern design techniques have been used [28]. The principal design parameters are collected in Table 4. It is seen that total physical thicknesses D_Σ of all 10 designs are close to each other, and the numbers of layers m are also close and vary from 38 to 44. Thicknesses of the thinnest layers $d_{\min}$ vary from 22.3 to 37.8 nm.

For each design, 1000 simulation runs were performed. In all simulations we used the monitoring strategy with the simple correction algorithm for TL and monitoring spreadsheets obtained using the novel algorithm. To form the monitoring spreadsheet, we first used the algorithm with a single monitoring wavelength and then, if the yield estimations were less than 90%, we increased the number of the wavelengths. For each design we also specified reasonable monitoring parameters from the following ranges: $a_1, b_1 \in [9;20]\% a_2, b_2 \in [80;91]\%$, and $\varepsilon \in [4;6]\%$, $\delta \in [4;6]\%$. If variations of parameters in these ranges did not help us to raise a production yield for the considered design, we excluded this design from consideration.

For production yield estimations the allowed ranges of transmittance were specified as follows: $T < 2\%$ in the spectral region from 425 to 670 nm, and $T > 94\%$ in the spectral region from 725 to 1200 nm (see Fig. 4). As a result, we found that the best solution is CM_6 (see Table 3). It exhibits a production yield of 100%, and its transmittance is also shown in Fig. 4. Solution CM_2 also shows high production yield of 99.7%. Production of both designs was simulated with monitoring at only one wavelength. In columns 3–6 of Table 3 we present monitoring parameters. In columns 7 and 8 of Table 3 we show monitoring wavelengths λ_{mon} and layers monitored at these wavelengths. In the last two columns of Table 3 we present estimations of production yields and their confidence levels. For the case of

Table 3. The Most Manufacturable Designs and Their Monitoring Parameters

Design	Number of Wavelengths	$S_{\text{in}} \times for \times a_1 \times$, b_1, %	$S_{\text{fin}} \times for \times a_2$, b_2, %	ε, %	δ, %	λ_{mon}, nm	Layers	Yield, %	Confidence Level, %
CM_6	1	20, 80	20, 80	4	4	790	all	100	0.3
CM_2	1	20, 80	20, 80	4	4	798	all	99.7	0.6
HM_7	1	15, 85	15, 85	6	6	697	all	100	0.3
BPF_1	1	20, 80	20, 80	4	4	500	all	96.3	1.6
BPF_5	1	20, 80	20, 80	4	4	500	all	98.7	1.0
TLF_1	1	10, 90	10, 90	6	6	549	all	98.8	0.9
EF_8	1	10, 90	10, 90	6	6	517	all	98.2	1.1
BS_4	3	9, 91	9, 91	6	6	565	1–12	96.0	1.6
						512	13–24		
						684	25–29		
BS_4	4	9, 91	9, 91	6	6	562	1–8	100	0.3
						525	9–16		
						732	17–24		
						684	25–29		

Table 4. Principal Design Parameters of CM Designs

Design	MF	m	D_Σ, nm	$d_{\min}$, nm
CM_1	0.4	40	3151.5	26.42
CM_2	0.4	44	3125.9	27.28
CM_3	0.5	42	3104.6	24.12
CM_4	0.6	42	3021.7	24.88
CM_5	0.4	44	3104.5	30.12
CM_6	0.5	38	2942.7	37.78
CM_7	0.4	44	3131.0	22.30
CM_8	0.5	40	2963.2	31.55
CM_9	0.6	42	2917.7	25.36
CM_10	0.5	40	2960.6	31.08

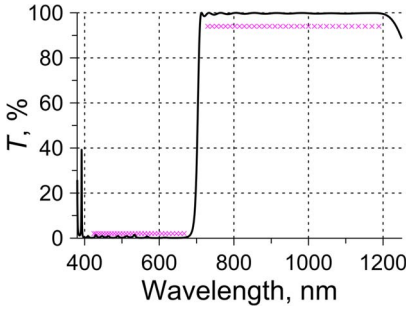

Fig. 4. Transmittance of design CM_6 (solid line) and Example 1 range target (magenta crosses).

computational manufacturing experiments the concept of confidence level is described in Ref. [29]. For designs CM_6 and CM_2, the monitoring wavelengths are located in the high transmittance spectral range but close to the transition region between this zone and the high reflection zone.

B. Example 2

Consider a problem of designing a hot mirror (HM). Target transmittance is 100% and 0% in the spectral ranges [400; 695] nm and [705; 1200] nm, respectively. Using various design algorithms, 10 solutions with numbers of layers from 38 to 48 and total physical thicknesses from 4190 to 5590 nm have been found. The main design parameters are collected in Table 5. It seems from Table 5 that design HM_8 is the most promising one because the thinnest layer has thickness of 85.4 nm. This layer is 4–7 times thicker than the thinnest layers of the other designs.

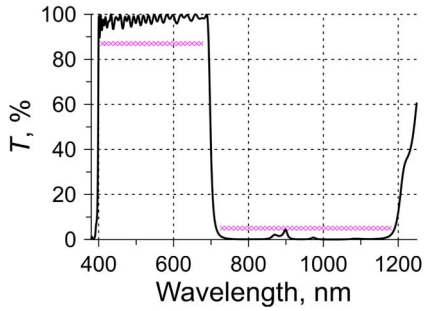

Fig. 5. Transmittance of design HM_7 (solid line) and Example 2 range target (magenta crosses).

At the same time the merit function, judging spectral performances of the designs, is maximal for the HM_8 solution.

Let us estimate production yields of the HM design solutions for the case when the novel strategy is used for generating monitoring spreadsheets. For computer simulations, the allowed ranges of transmittance are specified as $T > 87\%$ in the spectral region from 410 to 680 nm, and $T < 5\%$ in the spectral region from 730 to 1180 nm (the range target in Fig. 5). The simulations have shown that all designs except HM_7 exhibit very low production yields for a variety of monitoring parameters from MC2–MC5 and different numbers of monitoring wavelengths. Design HM_7 (Fig. 5) exhibits the highest production yield of 100% with single monitoring wavelength. This wavelength of 698 nm is located in the transmittance transition spectral range. This example shows that a design containing only thick layers is not necessarily more promising from the practical point of view.

C. Example 3

Consider a problem of designing a bandpass filter (BPF). Target transmittance is 100% in the spectral ranges from 400 to 495 nm and from 605 to 700 nm, and 0% in the spectral range [505; 595] nm. Different design methods provided 10 solutions with numbers of layers from 32 to 43 and total physical thicknesses from 2387 to 3429 nm. The principal design parameters of the 10 BPFs are collected in Table 6. In contrast to the CM and HM problems, the spectral transmittance of BPFs has not one but two transition zones, and the choice of monitoring wavelengths is

Table 5. Principal Design Parameters of HM Designs

Design	MF	m	D_Σ, nm	$d_{\min}$, nm
HM_1	2.9	40	4192.1	10.98
HM_2	0.97	48	5405.6	10.05
HM_3	1.37	48	5435.2	12.32
HM_4	1.83	48	5226.3	15.31
HM_5	1.88	46	5094.2	12.75
HM_6	1.97	48	5590.9	11.80
HM_7	1.5	38	4729.5	22.54
HM_8	3.24	40	5127.1	85.42
HM_9	2.33	40	4613.6	14.45
HM_10	2.33	42	4263.7	11.35

Table 6. Principal Design Parameters of BPF Designs

Design	MF	m	D_Σ, nm	$d_{\min}$, nm
BPF_1	0.70	38	3997.4	15.14
BPF_2	2.40	43	2826.7	10.33
BPF_3	0.97	42	2855.0	12.36
BPF_4	0.54	42	3176.1	15.06
BPF_5	0.94	32	3429.8	61.59
BPF_6	1.27	32	2804.6	17.22
BPF_7	1.30	32	2764.4	17.13
BPF_8	1.00	36	2706.9	13.34
BPF_9	1.54	34	3152.1	24.35
BPF_10	1.50	35	2387.1	14.65

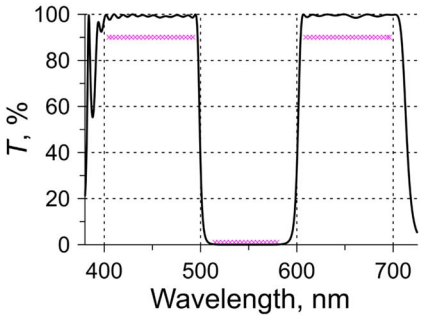

Fig. 6. Transmittance of design BPF_5 (solid line) and Example 3 range target (magenta crosses).

not evident. It is seen from Table 6 that the thinnest layer of design BPF_5 has thickness of 61.6 nm. This layer is 2–5 times thicker than the thinnest layers of the other designs. At the same time, the BPF_5 design has physical thickness of 3429.8 nm, which is larger than the thicknesses of almost all the other deigns.

To estimate production yields of the BPF designs, we specified allowed transmittance corridors as $T > 90\%$ in the spectral ranges from 405 to 493 nm and from 608 to 696 nm, and $T < 1\%$ in the spectral region from 515 to 580 nm (the range target in Fig. 6, where the transmittance of BPF_5 is also shown). Simulations have demonstrated that the BPF_1 and BPF_5 designs exhibit high production yields for the parameters shown in Table 3. It is shown that these high yield values can be achieved with a single monitoring wavelength. For both designs, the monitoring is to be performed at the wavelength of 500 nm from the first transition zone.

D. Example 4

Consider a problem of designing a three-line filter (TLF). Target transmittance is 100% in the spectral ranges [437; 459] nm, [510; 547] nm, and [599; 650] nm, and 0% in the spectral ranges [415; 430] nm, [465; 500] nm, [557; 588] nm, and [661; 780] nm. Using various design techniques, 10 solutions with numbers of layers from 36 to 48 have been obtained. The principal design parameters of these solutions can be found in Table 7. Spectral transmittances of the TLFs have four transition zones in the spectral range from 500 to 900 nm. As it was in the previous example, the choice of monitoring wavelengths is not evident.

It is seen from Table 7 that solutions TLF_4 and TLF_9 have maximal thicknesses of the thinnest layers: 35.2 and 30.1 nm, respectively. At the same time, these design have maximal total physical thickness of about 4850 nm and the maximal number of layers of 48. Designs TLF_5 and TLF_10 have the minimal numbers of layers—40 and 36, respectively—but contain thinner layers of 20.8 and 26.8 nm. Computer simulations allowed us to select a design that is the most promising for practical realization.

We perform simulations assuming that the thicknesses are controlled at the wavelengths found with the help of the novel strategy. The allowed transmittance corridors have been specified as $T > 90\%$ in the spectral ranges [440; 455] nm, [515; 545] nm, and [610; 645] nm, and $T < 5\%$ in the spectral regions [420; 427] nm, [470; 495] nm, [565; 580] nm, and [665; 780] nm (the range target in Fig. 7). Simulations have shown that TLF_1 (the transmittance shown in Fig. 7) provides a high production yield of 98.8% for the monitoring parameters shown in Table 3. This yield value can be achieved with only one monitoring wavelength. According to the novel strategy, the monitoring wavelength of 549 nm is located in the third transition zone.

E. Example 5

Consider a problem of designing an edge filter (EF). Target reflectance is 100% in the spectral ranges from 583 to 643 nm, and target transmittance is 100% in the spectral region from 610 to 710 nm. Incidence angle is 45 deg, and the light is unpolarized. Ten design solutions have been obtained with the help of various design methods. The main design parameters of these solutions are presented in Table 8. Spectral transmittances of EFs have transition zones, but these zones are different for a working angle of incidence of 45 deg and at the control angle of incidence close to 0 deg. Actually, the choice of monitoring wavelength(s) is not evident.

It is seen from Table 8 that, from the practical point of view, solutions EF_4, EF_5, EF_7, and EF_10 are the most attractive because they have maximal thicknesses of the thinnest layers. Designs EF_9 and EF_10 are also attractive because they

Table 7. Principal Design Parameters of TLF Designs

Design	*MF*	*m*	D_Σ, nm	$d_{\min}$, nm
TLF_1	1.49	49	3555.3	19.22
TLF_2	1.37	48	3964.2	19.66
TLF_3	0.81	49	4249.3	21.57
TLF_4	0.60	48	4853.3	35.18
TLF_5	1.32	40	4237.6	20.79
TLF_6	1.13	46	4227.3	26.00
TLF_7	1.14	43	4161.9	25.05
TLF_8	1.00	43	4210.3	23.00
TLF_9	0.66	48	4853.5	30.05
TLF_10	1.40	36	4217.1	26.78

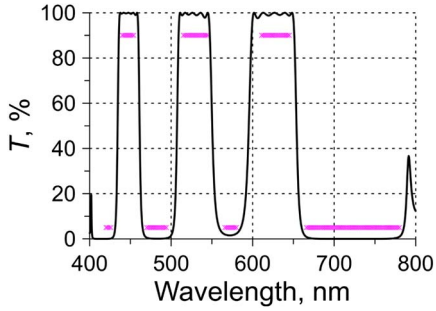

Fig. 7. Transmittance of design TLF_1 (solid line) and Example 4 range target (magenta crosses).

Table 8. Principal Design Parameters of EF Designs

Design	MF	m	D_Σ, nm	$d_{\min}$, nm
EF_1	0.94	29	3978.2	30.82
EF_2	1.14	27	3979.3	30.82
EF_3	0.67	32	4119.3	24.67
EF_4	0.63	30	3935.1	47.08
EF_5	0.96	28	3942.1	61.71
EF_6	1.25	29	3718.8	30.93
EF_7	1.04	26	4055.8	59.18
EF_8	0.67	29	3744.5	30.18
EF_9	1.67	25	3429.0	31.88
EF_10	2.08	24	4028.1	52.58

contain the smallest numbers of layers. Solution EF_10 has both advantages: a small number of layers, and the thickness of the thinnest layer is 52.6 nm. Computer simulations have given a key to reasonable choice of the combination [*design–strategy*].

We performed computational experiments assuming that the thicknesses are controlled at the wavelengths found with the help of the novel strategy. The range targets are T>93.5% in the spectral range [610; 710] nm, and R>99% in the spectral region [585; 638] nm (the range target in Fig. 8). Simulations have shown that the EF_7 design (its transmittance and reflectance shown in Fig. 8) provides the highest production yield of 100%, and solutions EF_1 and EF_8 provide high production yields of 99% and 98.6%, respectively. Evidently, designs EF_7 and EF_8 are more attractive for practical realization because they exhibit very high production yield with only one monitoring wavelength. It is interesting that the locations of the monitoring wavelengths found for EF_7 and EF_8 are not connected with the transition ranges of their spectral characteristics. Also, they are not close to each other.

F. Example 6

Consider a problem of designing a beam splitter (BS). Target reflectance is 50% for *s*- and *p*-polarized light in the spectral range from 620 to 680 nm, incidence angle is 45 deg, and the substrate's back side is included in the course of the design process. Ten

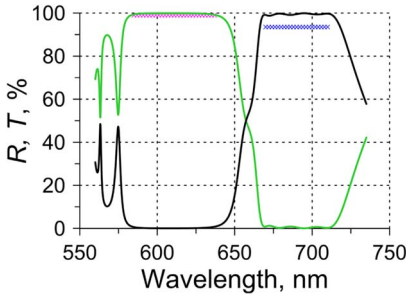

Fig. 8. Design EF_7: transmittance (solid black line) and reflectance (solid green line), and Example 5 range target (magenta crosses correspond to reflectance and blue crosses correspond to transmittance). The angle of incidence of nonpolarized light is 45 deg.

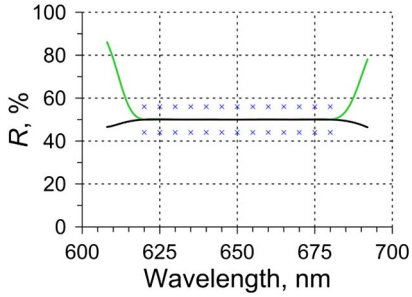

Fig. 9. Design BS_4 reflectances for *s*- (green solid line) and *p*-polarizations at 45 deg incidence; the blue crosses correspond to Example 6 range target.

different designs have been found with the help of several design methods. Reflectance of the design BS_4 is plotted in Fig. 9. The main design parameters of the solutions are presented in Table 9. Spectral characteristics of the BS designs have no transition zones in the working spectral range. A novel monitoring strategy can provide an appropriate sequence of monitoring wavelengths.

It is seen from Table 9 that there are no noticeable differences between obtained designs: the thinnest layers in all of them are not thinner than 30 nm, total physical thicknesses vary from 2966 to 3879 nm, and numbers of layers vary from 28 to 34. All solutions provide excellent approximations of target spectral characteristics (see merit function values in the first column of Table 9). Computer simulations can be used as a tool to find the best combination [*design–strategy*].

We performed experiments simulating deposition processes with the assumption that the layer thicknesses are monitored at the wavelengths found with the help of the novel strategy. The allowed corridor for reflectance data was from 44% to 56% in the working spectral range (Fig. 9). We found that, with the BS_4 solution and monitoring wavelengths computed by the novel strategy, high production yield of 99.6% and 100% can be achieved with three and four monitoring wavelengths, respectively. Other designs exhibit low or even zero production yield estimations. Therefore, in this case, the novel strategy also allows one to select the most manufacturable design for the cases when monochromatic monitoring is used for layer thicknesses control.

Table 9. Principal Design Parameters of BS Designs

Design	MF	m	D_Σ, nm	$d_{\min}$, nm
BS_1	0.12	31	3879.3	49.10
BS_2	0.20	31	3448.6	48.82
BS_3	0.21	28	3737.5	39.44
BS_4	0.03	29	3548.1	44.35
BS_5	0.26	27	2966.1	48.99
BS_6	0.05	34	3336.4	31.89
BS_7	0.29	29	3145.5	48.36
BS_8	0.33	34	3146.1	34.23
BS_9	0.02	34	3480.3	34.73
BS_10	0.37	29	3469.3	33.87

5. Conclusions

We proposed a new robust monochromatic monitoring strategy that takes into account practical requirements. The strategy allows one to form a sequence of monitoring wavelengths that contains a minimal number of wavelengths. We demonstrated that:

- the proposed algorithm allows one to generate a sequence of the specified number of monitoring wavelengths in such a way that the maximum possible number of practical conditions on swing and amplitude values as well as trigger point locations are satisfied;
- the novel strategy in combination with computer simulations allows one to select the practical parameters providing the highest production yield; and
- efficient design techniques in combination with the novel strategy and computer simulations provide an opportunity to find a series of design solutions and select the best [*design–strategy*] combinations in the assumption that the deposition process is controlled by monochromatic optical monitoring.

This work was supported by the DFG Cluster of Excellence, "Munich Centre for Advanced Photonics" (http://www.munich-photonics.de).

References

1. A. Tikhonravov, M. Trubetskov, and T. Amotchkina, "Optical monitoring strategies for optical coating manufacturing," in *Optical Thin Films and Coatings: From Materials to Applications*, Vol. **49** of Woodhead Publishing Series in Electronic and Optical Materials (Woodhead, 2013), pp. 62–93.
2. D. Ristau, H. Ehlers, T. Gross, and M. Lappschies, "Optical broadband monitoring of conventional and ion processes," Appl. Opt. **45**, 1495–1501 (2006).
3. S. Wilbrandt, O. Stenzel, N. Kaiser, M. K. Trubetskov, and A. V. Tikhonravov, "*In situ* optical characterization and reengineering of interference coatings," Appl. Opt. **47**, C49–C54 (2008).
4. B. Badoil, F. Lemarchand, M. Cathelinaud, and M. Lequime, "Interest of broadband optical monitoring for thin-film filter manufacturing," Appl. Opt. **46**, 4294–4303 (2007).
5. S. Waldner, R. Benz, P. Biedermann, and A. Jaunzens, "Broadband optical monitoring combined with additional rate measurement for accurate and robust coating processes," in *Optical Interference Coatings*, OSA Technical Digest (Optical Society of America, 2010), paper TuC10.
6. A. Zöller, M. Boos, H. Hagedorn, W. Klug, and C. Schmidt, "High accurate *in-situ* optical thickness monitoring," in *Optical Interference Coatings*, OSA Technical Digest (Optical Society of America, 2004), paper TuE10.
7. A. Zöller, M. Boos, H. Hagedorn, A. Kobiak, H. Reus, and B. Romanov, "Direct optical monitoring enables high performance applications in mass production," in *Optical Interference Coatings*, OSA Technical Digest (Optical Society of America, 2007), paper WC3.
8. A. Zöller, M. Boos, R. Götzelmann, H. Hagedorn, B. Romanov, and M. Viet, "Accuracy and error compensation with direct monochromatic monitoring," in *Optical Interference Coatings*, OSA Technical Digest (Optical Society of America, 2013), paper WB5.
9. M. Scherer, U. Schallenberg, H. Hagedorn, W. Lehnert, B. Romanov, and A. Zöller, "High performance notch filter coatings produced with PIAD and magnetron sputtering," Proc. SPIE **7101**, 71010I (2008).
10. A. Zöller, M. Boos, H. Hagedorn, and B. Romanov, "Computer simulation of coating processes with monochromatic monitoring," Proc. SPIE **7101**, 71010G (2008).
11. M. Gilo and D. Cohen, "Comparison of broad-band and single wavelength monitoring for IR coatings," in *Optical Interference Coatings*, OSA Technical Digest (Optical Society of America, 2013), paper WB4.
12. A. Zöller, M. Boos, R. Götzelmann, H. Hagedorn, and W. Klug, "Substantial progress in optical monitoring by intermittent measurement technique," Proc. SPIE **5963**, 59630D (2005).
13. A. V. Tikhonravov and M. K. Trubetskov, "Elimination of cumulative effect of thickness errors in monochromatic monitoring of optical coating production: theory," Appl. Opt. **46**, 2084–2090 (2007).
14. A. V. Tikhonravov, M. K. Trubetskov, and T. V. Amotchkina, "Statistical approach to choosing a strategy of monochromatic monitoring of optical coating production," Appl. Opt. **45**, 7863–7870 (2006).
15. A. V. Tikhonravov, M. K. Trubetskov, and T. V. Amotchkina, "Computational experiments on optical coating production using monochromatic monitoring strategy aimed at eliminating a cumulative effect of thickness errors," Appl. Opt. **46**, 6936–6944 (2007).
16. F. Zhao, "Monitoring of periodic multilayers by the level method," Appl. Opt. **24**, 3339–3342 (1985).
17. R. R. Willey and D. E. Machado, "Variation of band-edge position with errors in the monitoring of layer termination level for long- and short-wave pass filters," Appl. Opt. **38**, 5447–5451 (1999).
18. B. T. Sullivan and J. A. Dobrowolski, "Deposition error compensation for optical multilayer coatings. I. Theoretical description," Appl. Opt. **31**, 3821–3835 (1992).
19. C.-C. Lee, K. Wu, C.-C. Kuo, and S.-H. Chen, "Improvement of the optical coating process by cutting layers with sensitive monitoring wavelengths," Opt. Express **13**, 4854–4861 (2005).
20. C. Holm, "Optical thin film production with continuous reoptimization of layer thicknesses," Appl. Opt. **18**, 1978–1982 (1979).
21. B. Chun, C. K. Hwangbo, and J. S. Kim, "Optical monitoring of nonquarterwave layers of dielectric multilayer filters using optical admittance," Opt. Express **14**, 2473–2480 (2006).
22. T. V. Amotchkina, S. Schlichting, H. Ehlers, M. K. Trubetskov, A. V. Tikhonravov, and D. Ristau, "Computational manufacturing as a key element in the design–production chain for modern multilayer coatings," Appl. Opt. **51**, 7604–7615 (2012).
23. K. Friedrich, S. Wilbrandt, O. Stenzel, N. Kaiser, and K. H. Hoffmann, "Computational manufacturing of optical interference coatings: method, simulation results, and comparison with experiment," Appl. Opt. **49**, 3150–3162 (2010).
24. T. V. Amotchkina, M. K. Trubetskov, V. Pervak, and A. V. Tikhonravov, "Design, production, and reverse engineering of two-octave antireflection coatings," Appl. Opt. **50**, 6468–6475 (2011).
25. T. V. Amotchkina, S. Schlichting, H. Ehlers, M. K. Trubetskov, A. V. Tikhonravov, and D. Ristau, "Computational manufacturing as a tool for the selection of the most manufacturable design," Appl. Opt. **51**, 8677–8686 (2012).
26. A. V. Tikhonravov and M. K. Trubetskov, "OptiLayer software," http://www.optilayer.com.
27. S. A. Furman and A. V. Tikhonravov, *Basics of Optics of Multilayer Systems* (Editions Frontières, 1992).
28. A. V. Tikhonravov and M. K. Trubetskov, "Modern design tools and a new paradigm in optical coating design," Appl. Opt. **51**, 7319–7332 (2012).
29. A. V. Tikhonravov, M. K. Trubetskov, T. V. Amotchkina, and V. Pervak, "Estimations of production yields for selection of a practical optimal optical coating design," Appl. Opt. **50**, C141–C147 (2011).